

Plasma Membrane and Actin Cytoskeleton as Synergistic Barriers to Nanowire Cell Penetration

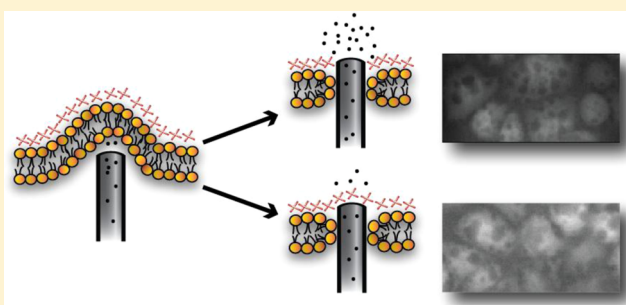
Amin Aalipour,[†] Alexander M. Xu,[†] Sergio Leal-Ortiz,[‡] Craig C. Garner,[‡] and Nicholas A. Melosh^{*,†}

[†]Department of Materials Science and Engineering, Stanford University, 476 Lomita Mall, Stanford, California 94305, United States

[‡]Department of Psychiatry and Behavioral Sciences, Stanford University, 1201 Welch Road, Stanford, California 94304, United States

S Supporting Information

ABSTRACT: Nanowires are a rapidly emerging platform for manipulation of and material delivery directly into the cell cytosol. These high aspect ratio structures can breach the lipid membrane; however, the yield of penetrant structures is low, and the mechanism is largely unknown. In particular, some nanostructures appear to defeat the membrane transiently, while others can retain long-term access. Here, we examine if local dissolution of the lipid membrane, actin cytoskeleton, or both can enhance nanowire penetration. It is possible that, during cell contact, membrane rupture occurs; however, if the nanostructures do not penetrate the cytoskeleton, the membrane may reclose over a relatively short time frame. We show with quantitative analysis of the number of penetrating nanowires that the lipid bilayer and actin cytoskeleton are synergistic barriers to nanowire cell access, yet chemical poration through both is still insufficient to increase long-term access for adhered cells.



INTRODUCTION

Interfacing living cells with arrays of vertically aligned, high aspect ratio nanostructures has become a rich field in nanobiotechnology.^{1–14} These systems allow for spatial and temporal control over large cell areas,¹ are adaptable across multiple cell types,^{2,3} and have been engineered to allow for electrical access^{4,5} and intracellular delivery.^{6–9} The utility of these systems derives from their ability to non-destructively deliver materials into cells, at least partially because of penetration through the cell membrane. Unknown or uncertain penetration still limits the use of these systems and necessitates techniques, such as electroporation^{5,9} or the use of cell permeabilizers,⁶ to ensure cell access. Thus, a fundamental understanding of the interactions that take place at the nanowire–cell interface is crucial to the design of such systems.

Two of the barriers for nanowire access are the plasma membrane, and the cytoskeleton, which consists of networks of intracellular scaffolding proteins, including microtubules, actin microfilaments, intermediate filaments, and spectrin. Much effort has been devoted to elucidating the role of the plasma membrane as a barrier to cell penetration,^{15–18} but the role of the actin cytoskeleton in this process remains unclear. Kagiwada et al. have presented data arguing that the insertion probability of a mechanically driven nanoneedle increases with a denser actin meshwork because the cytoskeleton acts as a rigid mechanical scaffold.¹⁹ Alternatively, a dense cytoskeletal network may prevent the nanostructure from entering the cell beyond the outer lipid bilayer, which could inhibit material delivery.

Here, we study the role of the plasma membrane and actin cytoskeleton as barriers to cell access in the context of nanostraw-mediated chemical delivery into living cells adhering onto the nanostructure array. We hypothesize that a nanowire or nanotube interacting with a cell is likely to adopt one of three configurations (Figure 1): (a) not penetrant and in contact with an intact lipid bilayer, (b) passing only through the cell membrane but not the cytoskeleton, or (c) passing through both the cell membrane and the cytoskeleton. The partially

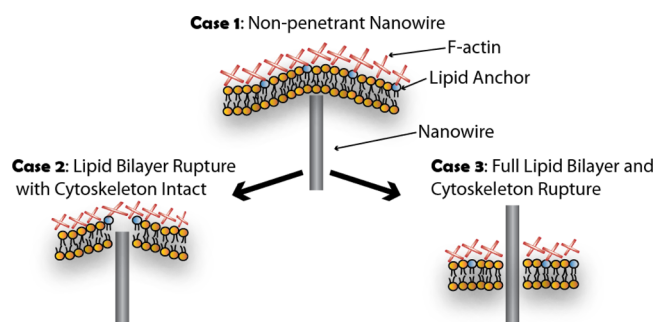


Figure 1. We hypothesize that high aspect ratio nanostructures that have penetrated into a cell can achieve one of two levels of cell access. These states may be important for intracellular delivery.

Received: June 11, 2014

Revised: September 13, 2014

Published: September 22, 2014

penetrating state may be more susceptible to closure of the lipid bilayer over the tube and elimination of continued cell access. For example, reassembly may be facilitated by the presence of exposed hydrophobic lipid anchors that, through interactions with other binding proteins, is fixed onto the intact cytoskeleton, such as phosphatidylinositol-4,5-bisphosphate (PIP₂).^{20–22} On the other hand, if the nanowire penetrated through both structures, there is much less incentive for the lipid membrane to reclose and may, thus, provide long-term access.

Previous work by our group introduced an engineered nanostraw array⁸ useful for quantifying the number of penetrant nanostructures (Figure 2A).²³ Molecules delivered in a

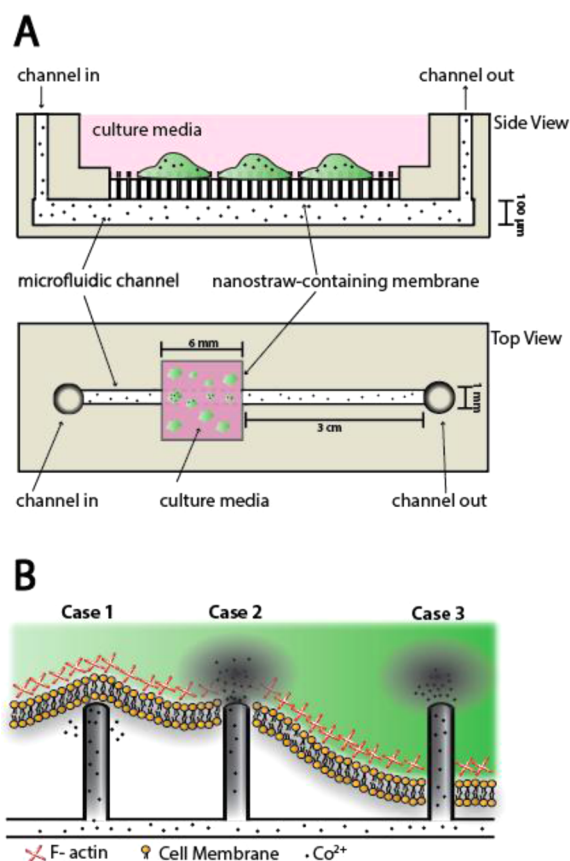


Figure 2. (A) The nanostraw platform allows for continuous fluidic access into cells via cell-penetrant nanotubes. (B) The Co^{2+} penetration assay offers a method of quantifying the number of nanostraws with cell access based on the number of puncta of fluorescence quenching observed in GFP-expressing cells. This assay allows us to gauge the effects of biochemical cell perturbations on adhered cells and determine how cytoskeleton integrity affects penetration frequency and delivery efficiency.

microfluidic channel beneath the nanostraws can move into cells via simple diffusion. This continuous fluidic access provides a potent method of cytosolic delivery for a vast array of biomolecules, including ions, protein, small molecules, and genetic material. Quantifying the number of penetrant nanostructures is achieved with a cobalt assay, wherein CoCl_2 is delivered into the microfluidic channel and Co^{2+} ions diffuse into green fluorescent protein (GFP)-expressing Chinese hamster ovary (CHO) cells cultured on a nanostraw device. Cobalt ions locally quench GFP fluorescence, which can be

visualized as dark spots forming in the cells (Figure 2B). Because these ions are membrane-impermeable, each puncta of quenching corresponds to the presence of a single penetrating nanostraw through which cobalt is being delivered. The number of spots in each cell can be divided by the product of the measured area of the cell and the density of nanostraws present on the membrane to obtain a normalized measure of penetration efficiency indicative of a nanostraw's level of cell access (Figure 2B).

Using the Co^{2+} penetration assay, we tested whether or not sequential dissociation of the plasma membrane and actin cytoskeleton could lead to gains in intracellular access by nanostraws. Chemical poration of the plasma membrane was achieved with the common biological solvent dimethyl sulfoxide (DMSO), which has the ability to increase membrane permeability through the formation of transient pores.^{24,25} Latrunculin A, a membrane-permeable drug that causes depolymerization of F-actin polymers by sequestering G-actin monomers,²⁶ was used to dissociate the actin cytoskeleton. Co-delivery of these dissociating agents along with the cobalt reporter can assess the role of the plasma membrane and actin cytoskeleton as barriers to cells adhering onto the nanostraw array.

EXPERIMENTAL SECTION

Microfluidic Device and Nanostraw Fabrication. Microfluidic devices were manufactured from polydimethylsiloxane (PDMS) as described previously.²³ Briefly, a nanostraw-containing membrane was sandwiched between a bottom piece of PDMS containing a fluidic channel, 1 mm wide and 100 μm deep, and a top piece of PDMS containing a volume for cell culture on the membrane (Figure 2A). Nanostraws ($\sim 1 \mu\text{m}$ height and $\sim 100 \text{ nm}$ diameter) were fabricated at the Stanford Nanofabrication Facility as previously described⁸ using polycarbonate membranes (Maine Manufacturing) with 100 nm diameter pores with a density of 0.3 pores μm^{-2} . Membranes were coated with $\sim 10 \text{ nm}$ of alumina using atomic layer deposition (Cambridge Nanotech), reactive ion etched with BCl_3/Cl_2 plasma to remove the top layer of alumina (Plasma Quest), and finally etched with O_2 plasma for 40 min at 100 W and $\sim 200 \text{ mTorr}$ to expose the alumina nanostraws (Plasma Prep III Solid State). Nanostraws were coated with polyornithine for 24 h prior to cell culture to enhance cell adhesion onto the nanostraws as previously described.²³

Cell Culture. CHO cells were transfected with eGFP plasmids using Lipofectamine, selected using 200 $\mu\text{g}/\text{mL}$ G418, and sorted using fluorescence-activated cell sorting (FACS) (Stanford Shared FACS Facility) at an intensity threshold of 3 orders of magnitude above null cells. Cells were maintained in Dulbecco's modified Eagle's medium with 10% fetal bovine serum and 1% penicillin/streptomycin. Trypsin–ethylenediaminetetraacetic acid (EDTA) (0.25%) was used to detach cells during plating. Reagents were purchased through Invitrogen.

Cobalt Penetration Assay. The cobalt penetration assay was performed by delivering 200 mM Co^{2+} prepared from CoCl_2 (Santa Cruz Biotechnology) dissolved in deionized water into the microfluidic channel below the nanostraws using syringe pumps operating at a flow rate of 0.1 mL h^{-1} . CHO cells were cultured at 500 cells mm^{-2} on the nanostraw device for 24 h prior to delivery. In co-delivery assays, DMSO (Fisher Scientific) and latrunculin A (Tocris Biosciences) were diluted to 2.5% (V/V) and 10 μM concentrations, respectively, in 200 mM Co^{2+} solution before delivery into the microfluidic channel. In experiments requiring sequential delivery of different solutions into the same channel, the channel was cleared by flowing phosphate-buffered saline (PBS) at a rate of 0.1 mL min^{-1} for 2 min through the channel. During delivery, fluorescence quenching with Co^{2+} was imaged at 20 \times magnification using epifluorescence on an inverted microscope (Zeiss). Images were collected at a rate of 0.1 Hz. Quenched puncta and cell area were counted and measured manually at snapshots 60–

90 s following delivery into the microfluidic channel (timepoints early enough to avoid overlapping puncta). Quenched puncta on the cell boundary are included in the analysis.

Statistical Analysis. In statistical analysis, each cell is considered an independent data point, and at least three separate experiments were performed for each condition described. Statistical significance was determined using a Student's *t* test.

RESULTS AND DISCUSSION

Delivery of different combinations of DMSO and latrunculin A along with a Co^{2+} reporter were used to determine how the lipid membrane and actin cytoskeleton affect nanostraw cell access (Figure 2B). An increase in fluorescence quenching from delivery of both DMSO and Co^{2+} in comparison to just Co^{2+} , for example, would suggest that the cell membrane is a barrier to ionic delivery that can be overcome with chemical poration. Similar experiments with only latrunculin A and Co^{2+} as well as the combination of DMSO, latrunculin A, and Co^{2+} were used to determine the effect of the actin cytoskeleton on delivery in the presence or absence of pores in the lipid bilayer.

Because systemic exposure to DMSO and latrunculin A is damaging to cell viability, we delivered these reagents through the nanostraws to localize them to the interface of the nanostraw and cell, where the effects would be greater with minimal global exposure. Further, we observed that delivery of only DMSO into the microfluidic channel at concentrations greater than 5% led to aberrant morphological changes in cells that would interfere with the puncta quantification in the cobalt assay (see Figure S1 of the Supporting Information). Thus, a DMSO concentration of 2.5% was selected to act as a mild permeabilizing agent while avoiding the extreme cell poration apparent at higher concentrations of DMSO. This approach differs from other reported studies using permeabilizing agents with nanotubes⁶ in that we purposely limit membrane poration to study possible interactions between the lipid bilayer and actin cytoskeleton.

When a solution of 200 mM Co^{2+} is delivered into the microfluidic channel after 24 h of cell culture on the device, we observe puncta of fluorescence quenching (Figure 3A) indicative of a baseline penetration frequency of 0.023 ± 0.0058 straws/ μm^2 . This frequency is equivalent to each individual nanostraw having on average a $7.7 \pm 1.9\%$ ($n = 140$) chance of piercing into a cell, consistent with previously reported values using the cobalt assay²³ (Figure 3B). Co-delivery of Co^{2+} in a solution of 2.5% DMSO leads to modest ($p < 0.001$) gains in intracellular Co^{2+} delivery, with a penetration efficiency of $8.8 \pm 2.0\%$ ($n = 49$; a 15% increase over baseline). This increase is consistent with the role of DMSO as a membrane permeabilizer as well as our use of a small concentration to limit excessive poration. While statistically significant, the majority (91.2%) of nanostraws still do not have intracellular access, hinting that the lipid bilayer alone is not the final arbiter of cellular access.

In contrast, co-delivery of Co^{2+} with 10 μM latrunculin A (without DMSO) does not result in any appreciable gain in penetration efficiency over the baseline with $7.9 \pm 2.4\%$ ($n = 99$) efficiency. We verified that latrunculin A (which is membrane-permeable) was acting on the cytoskeleton in that we observed cell blebbing (indicative of a loss of cytoskeleton integrity²⁷) upon prolonged delivery through the nanostraws (~ 20 min). Our findings suggest that, in our assay, the role of the actin cytoskeleton in mediating cell access is not appreciable as long as the lipid membrane is still intact. This is somewhat

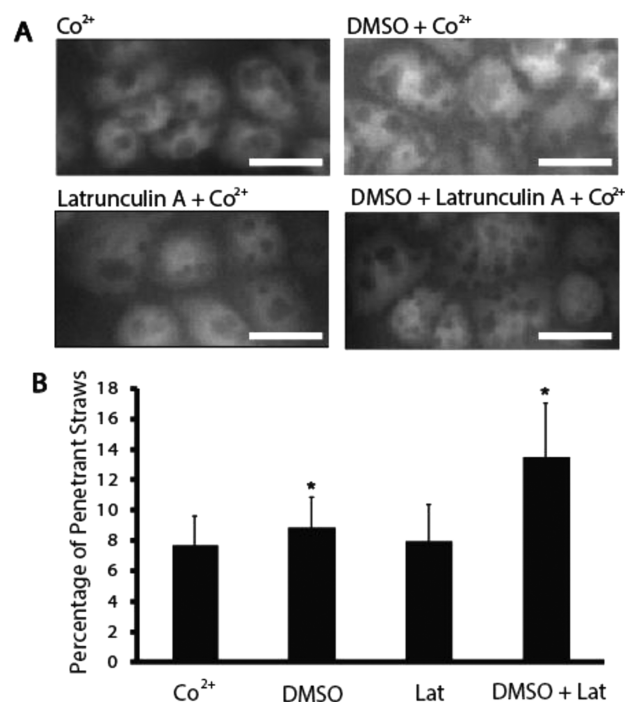


Figure 3. (A) Number of quenched fluorescence puncta seen in each condition are representative of the number of penetrant nanostraws in each cell. (B) Cobalt penetration assay enables quantification of penetration efficiency. Baseline penetration efficiency without cell perturbation is measured as $7.7 \pm 1.9\%$ ($n = 140$) and increases to $8.8 \pm 2.0\%$ ($n = 49$) with DMSO co-delivery. Co-delivery of latrunculin A with Co^{2+} shows no significant change in penetration efficiency ($7.9 \pm 2.4\%$; $n = 99$). Delivery of Co^{2+} with both DMSO and latrunculin A gives a penetration efficiency of $13.4 \pm 3.6\%$ ($n = 112$). Error bars depict standard deviation. (*) Statistically significant increase in penetration frequency over the baseline at the level of $p < 0.001$ using a Student's *t* test. Scale bar = 20 μm .

expected, given that Co^{2+} is highly membrane-impermeable and, thus, unlikely to enter cells without membrane disruption.

Surprisingly, co-delivery of both DMSO and latrunculin A with the cobalt reporter results in a dramatic spike in nanostraw penetration to $13.4 \pm 3.6\%$ ($n = 112$; 74% increase over baseline; $p < 10^{-30}$). This increase in efficiency is much higher than the increases associated with Co^{2+} co-delivery with DMSO or latrunculin A by themselves, demonstrating that the plasma membrane and actin cytoskeleton are synergistic barriers to intracellular access in adhered cells. Notably, the rate of delivery, measured as the time between Co^{2+} delivery and observation of fluorescence quenching inside cells, remains the same with or without chemical poration. The distributions of penetration frequency in each of the four conditions tested follow an approximately normal distribution (see Figure S2 of the Supporting Information).

These findings suggest that cell barriers to nanostraw access can be partially overcome with localized chemical poration. The localized delivery of latrunculin A, in particular, is important because complete dissociation of the actin cytoskeleton may interfere with cell adhesion onto the nanostructured surface.²⁸ In fact, non-localized (in the culture media) treatment of cells cultured on nanostraws with 10 μM latrunculin A for < 5 min causes a complete loss of all penetrant nanostraws in cells that exhibit a blebbing phenotype. This loss is potentially due to compromised actin-mediated adhesion and subsequent cell lift-

off from the nanostructured platform. In contrast, prolonged (~ 20 min) localized delivery of latrunculin A through the nanostraws does not affect penetrant nanostraws even when cells exhibit severe blebbing.

Reversibility of Chemical Poration. The cellular effects of both DMSO and latrunculin A are reversible,^{24,26} leading to the question of whether this localized dissociation of the membrane and cytoskeleton would lead to merely short-lived or permanent gains in nanostraw penetration. To study this, a pulse of Co^{2+} , DMSO, and latrunculin A (CDL) was delivered into the microfluidic channel, followed by a purging of the channel with PBS (Figure 4). After 10 min, a second pulse of

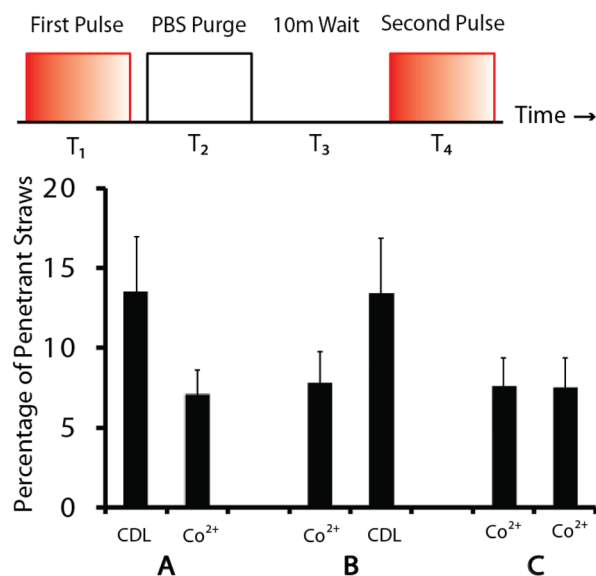


Figure 4. Reversibility of chemical poration is assessed by delivering two treatment pulses separated by a PBS purge and a 10 min wait. $T_1 = T_2 = T_4 = \sim 2$ min. (A–C) Penetration frequency of each of the two treatment pulses is shown for three separate experiments. (A) Effect of CDL exposure is reversible over this time scale, with the percentage of penetrant nanostraws reverting from $13.5 \pm 3.5\%$ ($n = 38$) to $7.1 \pm 1.6\%$ ($n = 30$). (B) There is no dependence upon pulse order because the percentage of penetrant straws increases from $7.8 \pm 2.0\%$ ($n = 100$) to $13.3 \pm 3.5\%$ ($n = 35$) in the CDL pulse. (C) This is confirmed in that two successive pulses of cobalt achieve penetration percentages of $7.6 \pm 1.8\%$ ($n = 40$) and $7.5 \pm 1.9\%$ ($n = 40$). Error bars depict standard deviation.

only Co^{2+} was delivered into the channel to determine whether the number of penetrant nanostraws remained at the high levels ($13.5 \pm 3.5\%$; $n = 38$) achieved with CDL delivery. We found that, even over this short time scale, the penetration efficiency reverts to baseline values ($7.1 \pm 1.6\%$; $n = 30$) during the second pulse (Figure 4A).

Our results also indicate that the local reassembly of the cell architecture occurs quickly and likely seals off the chemically porated nanostraws to prevent continued intracellular access. Additionally, this method of chemical poration does not appear to interfere with permanently penetrant straws because the second pulse of Co^{2+} still indicates baseline penetration levels. Morphological changes in cells because of latrunculin A would make it difficult to discern whether the “baseline” penetrant straws in the second pulse are the same permanently penetrant straws that exist before CDL treatment, but the similarity in penetration frequency suggests that this may be the case. A reversal of the order of the two pulses (Figure 4B) and two

staggered pulses of only Co^{2+} (Figure 4C) confirm that the order of delivery does not affect the frequency of penetration for each individual treatment.

This observation of cellular reassembly after chemical poration may be unique to the case of cells that have already adhered to the nanostraws. After 24 h of culture on the nanostraws, cells will have likely formed adhesive contacts between the lipid bilayer and the exterior of non-penetrant nanostraws, leading to relaxed cytoskeletal and membrane tension at the interface of the nanostraw and cell. These adhesive contacts would prevent changes in the membrane and cytoskeleton geometry around the nanostraw upon poration and explain why chemical poration does not lead to an increase in permanently penetrant nanostraws, because the lipids could “fill-in” directly into the membrane hole without changing the overall geometry. This would suggest that the observed permanently penetrant nanostraws may have a different configuration, such as case 3 in Figure 2B. These initially penetrant nanostraws would pierce through the lipid and actin cytoskeleton, leaving little reason for the lipid bilayer to extend over the nanostraw. Porating the lipid bilayer and cytoskeleton as cells first settle onto the nanostraws could in theory lead to more permanently penetrant nanostraws, but disruption of the cytoskeleton would likely impair formation of initial adhesive contacts with the nanostraw membrane that are a key driver of passive penetration.^{23,29}

Proposed Description of Nanostructure Penetration. Collectively, these results can be rationalized through a proposed description of nanostraw–cell interaction (Figure 5). When cells are simply cultured on nanostraws (panels A–C

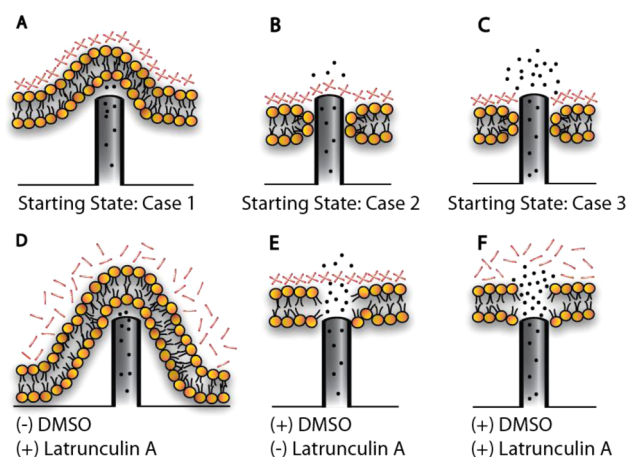


Figure 5. (A–C) Without chemical poration, (A) majority of nanostraws fails to gain intracellular access but (B) some are able to penetrate either the plasma membrane or (C) both the membrane and the cytoskeleton. (D) Treatment with latrunculin A does not cause any significant increase in penetration as long as the membrane is present, but (E) chemical poration of the membrane does lead to noticeable gains in cell access. (F) In contrast, chemical poration through both the membrane and the cytoskeleton leads to a drastic, non-additive increase in cell access.

of Figure 5), the majority of straws adopts the configuration in Figure 5A, wherein the actin cytoskeleton and plasma membrane prevent intracellular access. In this scenario, a small percentage of nanostraws adopts configurations shown in panels B and C of Figure 5, where permanent penetration is achieved by bypassing either the cell membrane or both the

membrane and the cytoskeleton, respectively. The fact that delivery of latrunculin A alone does not lead to appreciable gains in nanostraw penetration highly suggests that most of these permanently penetrating nanostraws exist in the state in Figure 5C. If this were not the case and many of the permanently penetrant nanostraws existed in the state in Figure 5B, then dissociation of the actin cytoskeleton would shift nanostraws to the state in Figure 5C and lead to a dramatic increase in penetration. This phenomenon is not observed with delivery of latrunculin A.

Chemical modifications can influence the interactions at the interface of the nanostraw and cell (panels D–F of Figure 5). Localized delivery of latrunculin A could convert a number of nanostraws in the state in Figure 5A to the state in Figure 5D, wherein the absence of a mechanically rigid cytoskeleton may cause changes in lipid bilayer morphology but no increased cellular access.¹⁹ In contrast, delivery of DMSO creates transient membrane pores that allow for an appreciable gain in intracellular access, such as in the geometry suggested in the state in Figure 5E. Localized delivery of both latrunculin A and DMSO could cause a transient state, such as in Figure 5F, which correlates with significantly enhanced intracellular access yet could easily lead to resealing.

This description of interaction at the interface of nanostraws and cells highlights potential limits to the efficiency of nanostructure-mediated intracellular delivery. In particular, while the plasma membrane is a relatively intuitive barrier to cell access, our results show that the actin cytoskeleton can indirectly impair delivery of even small ions into cells with porated membranes. It is possible that delivery of much larger structures, such as DNA or protein, may also be impaired by the cytoskeleton and that overcoming these barriers is important for achieving efficient delivery.

CONCLUSION

Using ionic delivery as a method of quantifying penetration frequency in adhered cells, we have shown that the plasma membrane and actin cytoskeleton are synergistic barriers to nanostraw access into a cell. These barriers can be reversibly overcome with localized chemical poration that acts as a “valve control” at the interface of the nanostraw and cell without interfering with already penetrant nanostructures. With the nanostraw platform, we are optimistic that these tools can be used to improve the efficiency of diffusion-based delivery for complex biological molecules. These results shed light on the relatively unstudied biological interactions at the interface of cells and high aspect ratio nanostructures and provide reason to consider barriers other than the plasma membrane when rationally engineering nanoplatforms for access into cells.

ASSOCIATED CONTENT

Supporting Information

Delivery of only DMSO into the microfluidic channel leads to morphological changes in cells in a concentration-dependent manner (Figure S1) and penetration frequency of all four experimental conditions follows an approximately normal distribution (Figure S2). This material is available free of charge via the Internet at <http://pubs.acs.org>.

AUTHOR INFORMATION

Corresponding Author

*E-mail: nmelosh@stanford.edu.

Notes

The authors declare no competing financial interest.

ACKNOWLEDGMENTS

The authors thank members of the Sarah Heilshorn laboratory and Yi Cui laboratory for use of equipment. Part of this work was performed at the Stanford Nano Shared Facilities (SNSF). This work was funded by NSF IDBR-1063397 and Stanford NeuroVentures. Alexander M. Xu was supported by a National Science Foundation (NSF) graduate fellowship and National Defense Science and Engineering Graduate (NDSEG) fellowship.

REFERENCES

- (1) El-Ali, J.; Sorger, P. K.; Jensen, K. F. Cells on chips. *Nature* **2006**, *442*, 403–411.
- (2) Kim, W.; Ng, J. K.; Kunitake, M. E.; Conklin, B. R.; Yang, P. Interfacing silicon nanowires with mammalian cells. *J. Am. Chem. Soc.* **2007**, *129*, 7228–7229.
- (3) Xie, C.; Hanson, L.; Xie, W.; Lin, Z.; Cui, B.; Cui, Y. Noninvasive neuron pinning with nanopillar arrays. *Nano Lett.* **2010**, *10*, 4020–4024.
- (4) Cohen-Karni, T.; Timko, B. P.; Weiss, L. E.; Lieber, C. M. Flexible electrical recording from cells using nanowire transistor arrays. *Proc. Natl. Acad. Sci. U. S. A.* **2009**, *106*, 7309–7313.
- (5) Xie, C.; Lin, Z.; Hanson, L.; Cui, Y.; Cui, B. Intracellular recording of action potentials by nanopillar electroporation. *Nat. Nanotechnol.* **2012**, *7*, 185–190.
- (6) Peer, E.; Artzy-Schnirman, A.; Gepstein, L.; Sivan, U. Hollow nanoneedle array and its utilization for repeated administration of biomolecules to the same cells. *ACS Nano* **2012**, *6*, 4940–4946.
- (7) Shalek, A. K.; Robinson, J. T.; Karp, E. S.; Lee, J. S.; Ahn, D.-R.; Yoon, M.-H.; Sutton, A.; Jorgolli, M.; Gertner, R. S.; Gujral, T. S.; MacBeath, G.; Yang, E. G.; Park, H. Vertical silicon nanowires as a universal platform for delivering biomolecules into living cells. *Proc. Natl. Acad. Sci. U. S. A.* **2010**, *107*, 1870–1875.
- (8) VanDersarl, J. J.; Xu, A. M.; Melosh, N. A. Nanostraws for direct fluidic intracellular access. *Nano Lett.* **2012**, *12*, 3881–3886.
- (9) Xie, X.; Xu, A. M.; Leal-Ortiz, S.; Cao, Y.; Garner, C. C.; Melosh, N. A. Nanostraw–electroporation system for highly efficient intracellular delivery and transfection. *ACS Nano* **2013**, *7*, 4351–4358.
- (10) Fan, D.; Yin, Z.; Cheong, R.; Zhu, F. Q.; Cammarata, R. C.; Chien, C. L.; Levchenko, A. Subcellular-resolution delivery of a cytokine through precisely manipulated nanowires. *Nat. Nanotechnol.* **2010**, *5*, 545–551.
- (11) Persson, H.; Beech, J. P.; Samuelson, L.; Oredsson, S.; Prinz, C. N.; Tegenfeldt, J. O. Vertical oxide nanotubes connected by subsurface microchannels. *Nano Res.* **2012**, *5*, 190–198.
- (12) Almquist, B. D.; Melosh, N. A. Fusion of biomimetic stealth probes into lipid bilayer cores. *Proc. Natl. Acad. Sci. U. S. A.* **2010**, *107*, 5815–5820.
- (13) Park, J.; Bauer, S.; von der Mark, K.; Schmuki, P. Nanosize and vitality: TiO₂ nanotube diameter directs cell fate. *Nano Lett.* **2007**, *7*, 1686–1691.
- (14) Na, Y.-R.; Kim, S. Y.; Gaublomme, J. T.; Shalek, A. K.; Jorgolli, M.; Park, H.; Yang, E. G. Probing enzymatic activity inside living cells using a nanowire–cell “sandwich” assay. *Nano Lett.* **2013**, *13*, 153–158.
- (15) Berthing, T.; Bonde, S.; Rostgaard, K. R.; Madsen, M. H.; Sorensen, C. B.; Nygård, J.; Martinez, K. L. Cell membrane conformation at vertical nanowire array interface revealed by fluorescence imaging. *Nanotechnology* **2012**, *23*, 415102.
- (16) Hanson, L.; Lin, Z. C.; Xie, C.; Cui, Y.; Cui, B. Characterization of the cell–nanopillar interface by transmission electron microscopy. *Nano Lett.* **2012**, *12*, 5815–5820.

- (17) Liu, F.; Wu, D.; Kamm, R. D.; Chen, K. Analysis of nanoprobe penetration through a lipid bilayer. *Biochim. Biophys. Acta* **2013**, *1828*, 1667–1673.
- (18) Mumm, F.; Beckwith, K. M.; Bonde, S.; Martinez, K. L.; Sikorski, P. A transparent nanowire-based cell impalement device suitable for detailed cell–nanowire interaction studies. *Small* **2013**, *9*, 263–272.
- (19) Kagiwada, H.; Nakamura, C.; Kihara, T.; Kamiishi, H.; Kawano, K.; Nakamura, N.; Miyake, J. The mechanical properties of a cell, as determined by its actin cytoskeleton, are important for nanoneedle insertion into a living cell. *Cytoskeleton* **2010**, *67*, 496–503.
- (20) Saarikangas, J.; Zhao, H.; Lappalainen, P. Regulation of the actin cytoskeleton–plasma membrane interplay by phosphoinositides. *Physiol. Rev.* **2010**, 259–289.
- (21) Skrzyny, M.; Brach, T.; Ciuffa, R.; Rybina, S.; Wachsmuth, M.; Kaksonen, M. Molecular basis for coupling the plasma membrane to the actin cytoskeleton during clathrin-mediated endocytosis. *Proc. Natl. Acad. Sci. U. S. A.* **2012**, *109*, E2533–42.
- (22) Itoh, T.; Koshiba, S.; Kigawa, T.; Kikuchi, A.; Yokoyama, S.; Takenawa, T. Role of the ENTH domain in phosphatidylinositol-4,5-bisphosphate binding and endocytosis. *Science* **2001**, *291*, 1047–1051.
- (23) Xu, A. M.; Aalipour, A.; Leal-Ortiz, S.; Mekhdjian, A. H.; Xie, X.; Dunn, A. R.; Garner, C. C.; Melosh, N. A. Quantification of nanowire penetration into living cells. *Nat. Commun.* **2014**, *5*, 1–8.
- (24) Gurtovenko, A. A.; Anwar, J. Ion transport through chemically induced pores in protein-free phospholipid membranes. *J. Phys. Chem. B* **2007**, *111*, 13379–13382.
- (25) De Ménorval, M.-A.; Mir, L. M.; Fernández, M. L.; Reigada, R. Effects of dimethyl sulfoxide in cholesterol-containing lipid membranes: A comparative study of experiments in silico and with cells. *PLoS One* **2012**, *7*, No. e41733.
- (26) Coué, M.; Brenner, S.; Spector, I.; Korn, E. Inhibition of actin polymerization by latrunculin A. *FEBS Lett.* **1987**, *2*, 316–318.
- (27) Fackler, O. T.; Grosse, R. Cell motility through plasma membrane blebbing. *J. Cell Biol.* **2008**, *181*, 879–884.
- (28) Parsons, J. T.; Horwitz, A. R.; Schwartz, M. A. Cell adhesion: Integrating cytoskeletal dynamics and cellular tension. *Nat. Rev. Mol. Cell Biol.* **2010**, *11*, 633–643.
- (29) Xie, X.; Xu, A. M.; Angle, M. R.; Tayebi, N.; Verma, P.; Melosh, N. A. Mechanical model of vertical nanowire cell penetration. *Nano Lett.* **2013**, *13*, 6002–6008.